Int. J. Electrochem. Sci., 8 **(2013)** 5496 - 5505

International Journal of
ELECTROCHEMICAL
SCIENCE
www.electrochemsci.org

Effect of Electrodeposition Parameters on the Current Density of Hydrogen Evolution Reaction in Ni and Ni-MoS_2 Composite Coatings

E. Saraloğlu Güler[1,*], *E. Konca*[2] *and İ. Karakaya*[1]

[1] Department of Metallurgical and Materials Engineering, Middle East Technical University, Ankara, TURKEY
[2] Department of Metallurgical and Materials Engineering, Atilim University, Incek, Ankara, TURKEY
[*]E-mail: saebru@metu.edu.tr

Received: 10 September 2012 / *Accepted:* 26 February 2013 / *Published:* 1 April 2013

Nickel composites with co-deposited insoluble, solid lubricant particles such as MoS_2 have been reported to reduce friction. It is known that hydrogen evolution reaction (HER), competes with nickel deposition. The influence of the parameters and their interaction effects on the peak current density of HER during the electrodeposition of Ni and Ni-MoS_2 composite coatings were studied by fractional factorial design. The parameters and their ranges studied were; MoS_2 particle concentration (0-30 g/l), temperature (30-50ºC), pH (2-4) and two surfactants, namely; ammoniumlignosulfonate (ALS) and depramin-C (DC) (0-1 g/l). Electrodeposition processes were carried out from a typical Watts bath containing leveler, wetting agent and brightener by using a potentiostat. The peak current densities (i_p) were extended to higher values and the peaks on linear sweep voltammograms became noticeable by increasing the scan rate from 20 mV/s to 100 mV/s over the range of 0 to 2.5 V. The peak current densities (i_p) of HER for each experimental route were determined by fractional factorial design for two mineral processing surfactants; ammoniumlignosulfonate (ALS) and depramin-C (DC) using a statistical analysis software named Minitab [1]. Adding MoS_2, decreasing temperature and increasing pH had decreasing effects on the peak current density of HER regardless of the surfactant used. On the other hand, the surfactants increased the peak current density.

Keywords: Hydrogen evolution reaction, Ni, MoS_2, fractional factorial design, electroplating, electrocodeposition, current density

1. INTRODUCTION

The composite deposition of insoluble solid particles embedded in a metal matrix has been offered for several industrial applications. Composite coatings based on nickel with build-in lubricant

particles such as; BN [1, 2], MoS_2 [3-6], *polytetrafluoroethylene* (PTFE) [7, 8], and graphite [9, 10] were produced to have improved tribological behavior. The effects of electrodeposition parameters such as current density, concentration of MoS_2 in electrolyte, pH, temperature, stirring rate and surfactant concentration on the amount of MoS_2 deposited in the MoS_2-Ni composite coatings were investigated [4, 6]. Fractional factorial design was used to evaluate the influence of all or some of the above parameters and also the complex interactions on corrosion resistance, deposition efficiency [11] and hydrogen evolving activity [12, 13].

Hydrogen evolution on the cathode together with nickel makes electrodeposited coatings susceptible of hydrogen adsorption which then affects materials behavior in service, decreases current efficiency and leads to a dull and nonuniform surface. The electrodeposition parameters influence hydrogen evolution reaction (HER) and thus hydrogen permeation in nickel. However, these parameters may also alter the crystal texture, defects present, grain size and internal stress which in turn can change diffusion and trapping of hydrogen in nickel [14]. Texture formation in nickel deposits has been attributed to HER by Fritz et. al. [15] who claimed that increasing mean current density changes texture from (110) to (100). The relationship between texture and current density together with the pH of Watts' electrolyte was in general agreement [16], but there are some differences in the values of the current densities. At low current densities, the (110) texture was favored due to the inhibition of growth which was attributed to hydrogen adsorption [17] whereas (100) texture was observed at the high current densities because of uninhibited growth (free growth mode) of nickel [15, 16, 18].

In practice, strike nickel coatings are performed at low current densities for stronger bonding [19-22]. This can be attributed to the hydrogen codeposition that favors the (110) texture. The low current density application in nickel plating was also reported to assist bonding process in electronic packaging [19].

It is expected that strong bonding of MoS_2 particles to the nickel matrix may be achieved by producing nickel coating that favors (110) texture, which would assist to have longer service life for the electrodeposited composite coatings. For this reason, attention was turned to the effects of plating parameters on the hydrogen evolution during the electrodeposition of Ni and Ni-MoS_2 composite coatings by fractional factorial design. Two commonly used anionic mineral processing surfactants; ammoniumlignosulfonate (ALS) (66071-92-9; Tembec, Canada) and depramin-C (DC) (9004-32-4; Akzo, Netherlands) were used [23, 24] to test their effects on HER. Further, interaction effects for the parameters were evaluated.

2 EXPERIMENTAL

A typical Watts bath (300 g/l $NiSO_4.6H_2O$ (63035981; Umicore, Belgium), 50 g/l $NiCl_2.6H_2O$ (7791-20-0; Selnic, France), and 40 g/l boric acid (minimum %99.9 H_3BO_3, Etibank, Turkey) was used for the study. The electrolyte bath was prepared by dissolving above components in deionized water at 60°C according to procedure given in Surtec 855 [25]. The following additives; 4 ml/l carrier (SurTec

850), 10 ml/l leveler (SurTec 855), 1 ml/l brighthener (SurTec 855), and 1 ml/l wetting agent (SurTec 850) were added to the bath to simulate a typical nickel plating solution.

After immersion into an alkaline solution and anodic acid cleaning to produce clean surface required for electrodeposition [26-28], AISI 304 stainless steel (EN 10204) substrates of 40x40x0.5 mm were placed in the electrodeposition cell schematically shown in Fig. 1. They were placed into the electrolyte to have only 10 cm^2 exposed area. Stainless steel cathode (working electrode) was connected to W pole, while nickel anode (counter electrode and acting as reference electrode at the same time) was connected to both C and R poles of a GAMRY Reference 3000 Potentiostat.

To identify the effects of 5 electrodeposition variables on hydrogen evolution profile with the reasonable number of experiments, 2^{5-1} fractional factorial design, regression analysis and mixture design were used. The variables were determined as; A: MoS_2 (Merck-product no: 1122570250) concentration, B: Temperature, C: pH, D: Surfactant, E: Coating thickness. The levels of above variables are given in Table 1. Low and high level values of the parameters were selected based on the previous studies in the literature [3, 4, 6]. The experimental route obtained by 2^{5-1} fractional factorial design using the statistical analysis software Minitab [29] is given in Table 2. The peak current density (i_p) and the peak voltage (V_p) values in the process were chosen as the response values in the design.

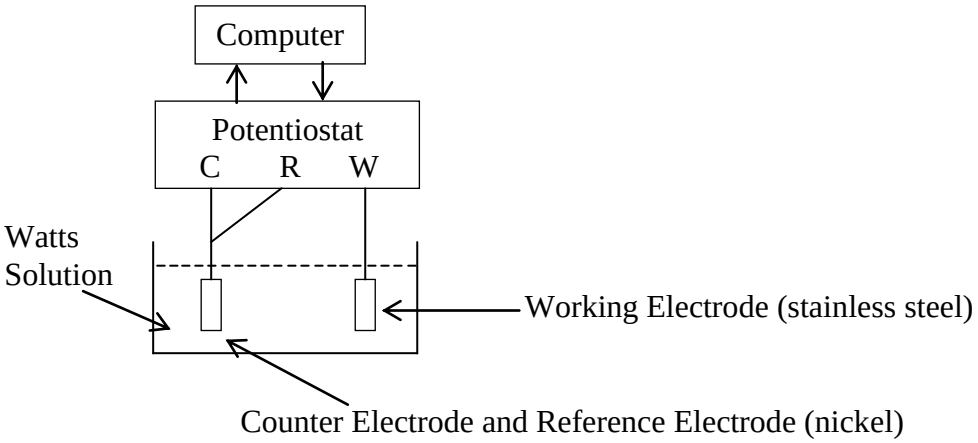

Figure 1. Schematic view of the electrodeposition set-up. W, C and R are poles for working, counter and reference electrodes respectively.

Table 1. Factors and Levels for Fractional Factorial Design (FFD)

Factor	Designation	Levels	
		-1	+1
MoS_2 concentration (g/l)	A	0	30
Temp(°C)	B	30	50
pH	C	2	4
Surfactant (g/l)	D	0	1
Coating Thickness (μm)	E	0	40

The voltammetric responses between the working electrode (cathode) and the nickel anode were recorded during electrodeposition of nickel and Ni-MoS_2 composite coatings from Watts' bath according to the conditions given in Table 2. The potentials were swept linearly from 0 to 2.5 V at two different scan rates of 20 mV/s and 100 mV/s. "Echem Analyst" program was used to determine the i_p and V_p values associated with HER.

Table 2. Experimental conditions for 2^{5-1} Fractional Factorial Design: -1 = low values 1 = high values for the variables

Experiment #	A (MoS_2)	B (Temp.)	C (pH)	D (Surfactant)	E (Thickness)
1	-1	-1	-1	-1	1
2	-1	1	1	-1	1
3	1	-1	-1	1	1
4	1	1	-1	-1	1
5	1	1	1	1	1
6	-1	-1	1	1	1
7	1	-1	1	-1	1
8	-1	1	-1	1	1
9	1	1	-1	1	-1
10	1	-1	-1	-1	-1
11	-1	1	-1	-1	-1
12	-1	1	1	1	-1
13	-1	-1	-1	1	-1
14	1	1	1	-1	-1
15	-1	-1	1	-1	-1
16	1	-1	1	1	-1

3. RESULTS AND DISCUSSION

The effect of scan rate on the voltammogram is illustrated in Fig. 2 for experiment 2 under conditions given in Table 2. It is apparent that total current density at extremum increases with increasing scan rate as expected [30]. Therefore, 100 mV/s was chosen as the scan rate in the successive experiments since i_p's were well determined and predominant when potential scan rate increased. From Fig. 2, it can be seen that the current density is almost zero until the onset of reduction of nickel and/or hydrogen ions at the cathode. Then, it continually increases and reaches a maximum. The irregularity of the voltammogram after the maximum indicates the decay of one of the primary electrode reactions.

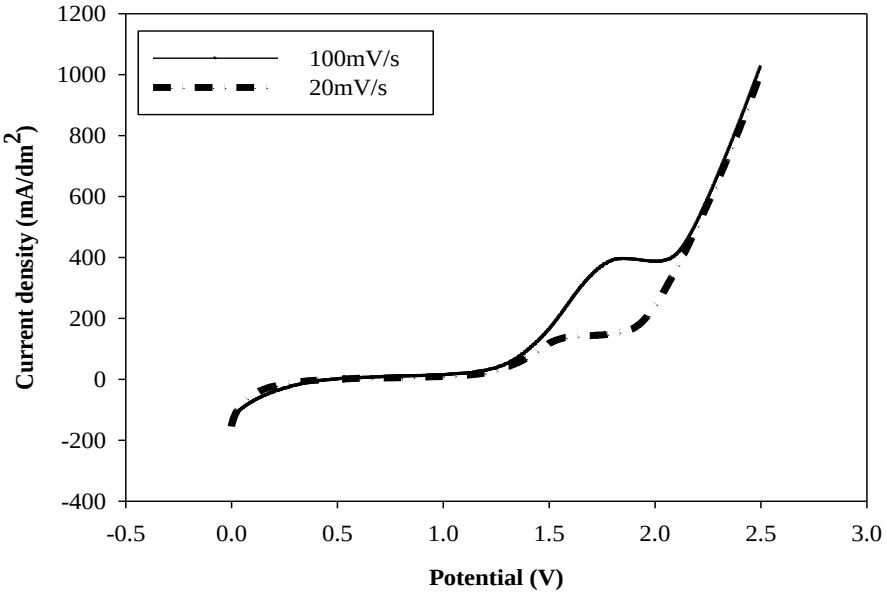

Figure 2. The effect of scan rate on the voltammogram for experiment 2 under conditions given in Table 2

Table 3. I_p (cathode 10 cm^2), V_p and i_p values for experiments from 1 to 16

Experiment #	Surfactant	I_p (A)	V_p (V)	i_p (A/dm^2)
1	-	0.07040	2.323	0.704
2	-	0.03950	1.861	0.395
3	DC	0.05772	1.926	0.577
	ALS	0.06210	2.059	0.621
4		0.07079	2.160	0.708
5	DC	0.03944	1.879	0.394
	ALS	0.05628	1.728	0.563
6	DC	0.02672	1.865	0.267
	ALS	no peak	no peak	no peak
7	-	no peak	no peak	no peak
8	DC	0.01056	1.915	0.106
	ALS	0.01412	2.142	0.141
9	DC	0.05273	1.686	0.527
	ALS	0.04745	1.716	0.474
10	-	0.03090	1.609	0.309
11	-	0.07180	2.023	0.718
12	DC	0.02182	1.498	0.218
	ALS	0.02053	1.535	0.205
13	DC	0.04153	1.676	0.415
	ALS	0.04187	1.719	0.419
14	-	0.03243	1.649	0.324
15	-	0.01989	1.595	0.199
16	DC	0.02084	1.592	0.208
	ALS	0.03631	1.706	0.363

To test the decay of HER, current efficiencies of nickel plating were determined at 3 different current densities selected from the voltammogram. One of the selected current density values was the peak value. The other two were the values before and after the peak value. Under the conditions of experiment 15, for 2 and 8 hours of depositions, the average current efficiency for nickel were determined as 90%, nearly 100% and 68% for the current densities before, after and at the peak value, respectively. The decrease in the current efficiency at the peak position can be attributed to the HER since cathodic current efficiency of nickel deposition in Watts' bath decreases due to the hydrogen evolution at a current density of about 0.65 A/dm^2 [31]. As shown in Table 3, the peak current densities obtained are comparable with the study of Ibrahim [31].

The typical volammograms and the positions of i_p values for the first four experiments are shown in Fig. 3. The values of the peak current, I_p, the peak current density, i_p, and the peak voltage, V_p, together with surfactant designations are given in Table 3 for all experiments.

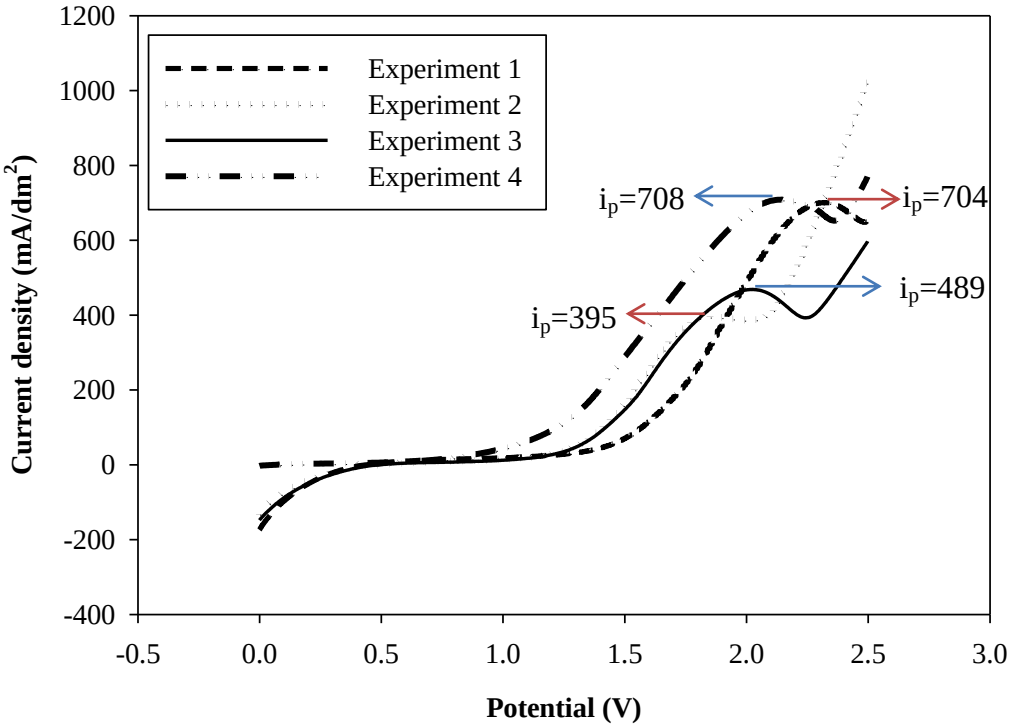

Figure 3. The typical voltammograms at 100 mV/s scan rate and the positions of i_p values, in mA/dm^2, for the first four experiments

The results were subjected to factorial design analysis to obtain the interaction effects of surfactants as illustrated in Fig. 4. Only four parameters were used in the analysis since the coating thickness has no effect on the current density. The parameters that have decreasing effect on the current density yielded negative coefficients in the regression analysis (Equations 1 and 2 below) and the magnitudes of the coefficients indicate the weights of their effects. The corresponding surfactant for each equation is given inside the parenthesis next to the equations.

$$i_p\ (mA/dm^2) = 557 - 48.6\ A + 81.4\ B - 204\ C + 16.7\ D \qquad (DC) \qquad (1)$$

$$i_p\ (mA/dm^2) = 675 - 113\ A + 95\ B - 186\ C + 135\ D \qquad (ALS) \qquad (2)$$

The variables A, B, C and D in above equations are already presented with their units in Table 1. It can be concluded that parameters A (MoS_2) and C (pH) have decreasing while the parameter B (temperature) has increasing effect on the peak current density regardless of the surfactant used. The decrease in i_p with MoS_2 particles (A) may be explained by the adsorption of positively charged hydrogen ions in solution on negatively charged MoS_2 particles [3, 32]. Particles with adsorbed ions move to cathode where H^+ ions are reduced to hydrogen gas. This adsorption will end up with heavy weight couples which lead to decrease in mobility and thus increase in polarization. The increase in pH, in other words; the decrease in the concentration of hydrogen ions will decrease the rate of the hydrogen gas evolution reaction that will lead to diminishing effect on i_p. Since the temperature improves ion diffusion rate, i_p was increased due to retardation in polarization. Using ALS and DC increased the peak current density. However, the weight of surfactant effect in ALS is more significant compared to DC. Voltammetric response was apparently improved with decreasing the overpotential in the presence of anionic surfactants [33, 34] and the peak current density values for H^+ reduction were increased. This is in accord with the expectations that anionic surfactants can promote both oxidation and reduction processes [35].

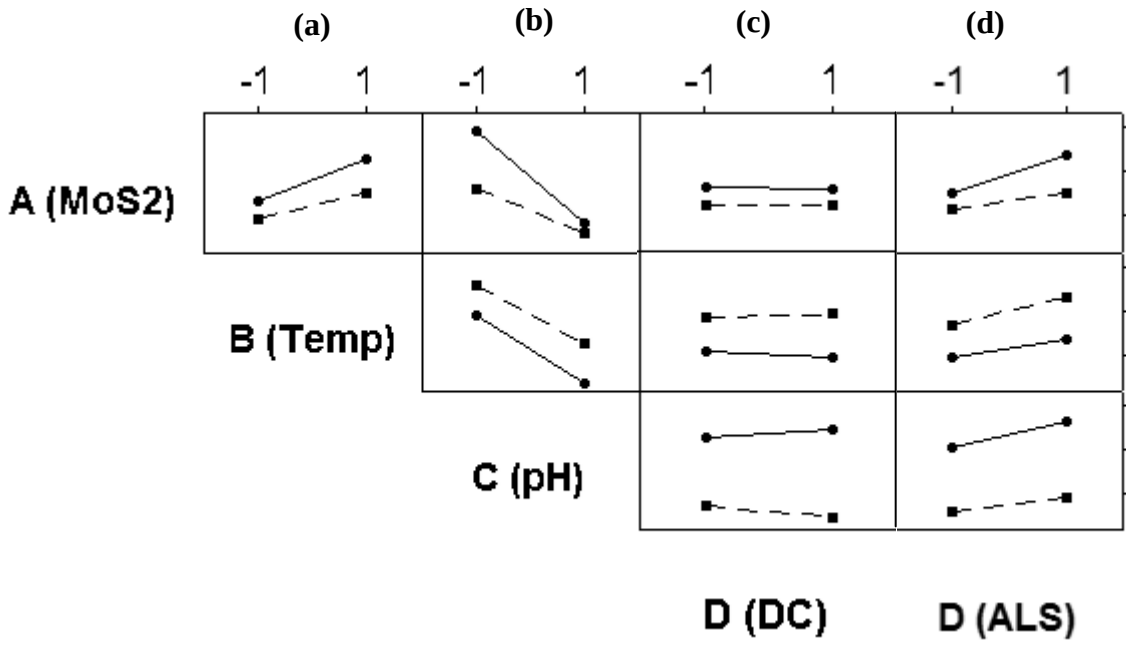

Figure 4. Interaction plot for peak current densities; the columns are showing; **(a)** A-B **(b)** A-C and B-C **(c)** A-D, B-D and C-D interactions for Surfactant DC and **(d)** for Surfactant ALS. The dashed and full lines in this figure represent high and low levels respectively. The i_p scales of vertical axes are not shown for simplicity.

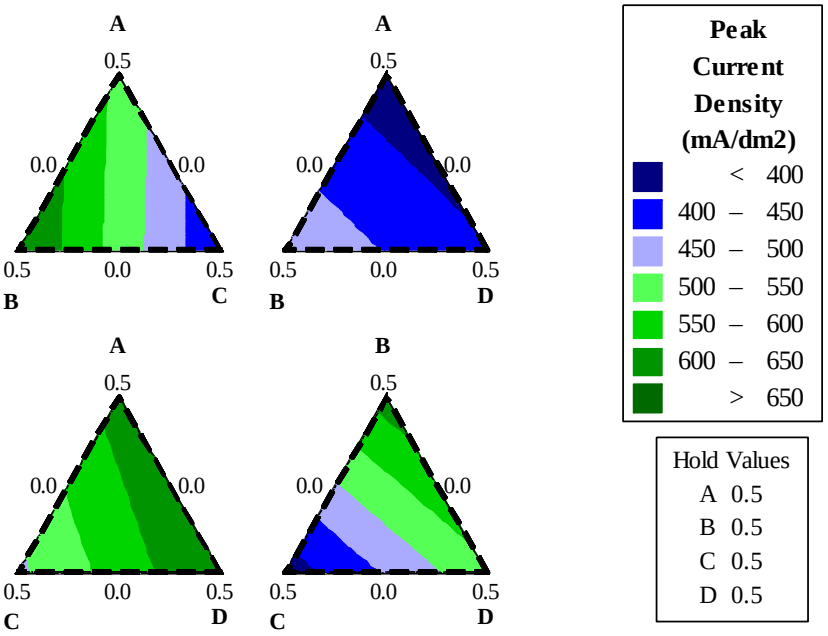

Figure 5. Matrix of mixture contour plots for the peak current densities (mA/dm^2) when surfactant DC was used. The parameters are; **A** (MoS_2), **B** (Temp.), **C** (pH), **D** (Surfactant).

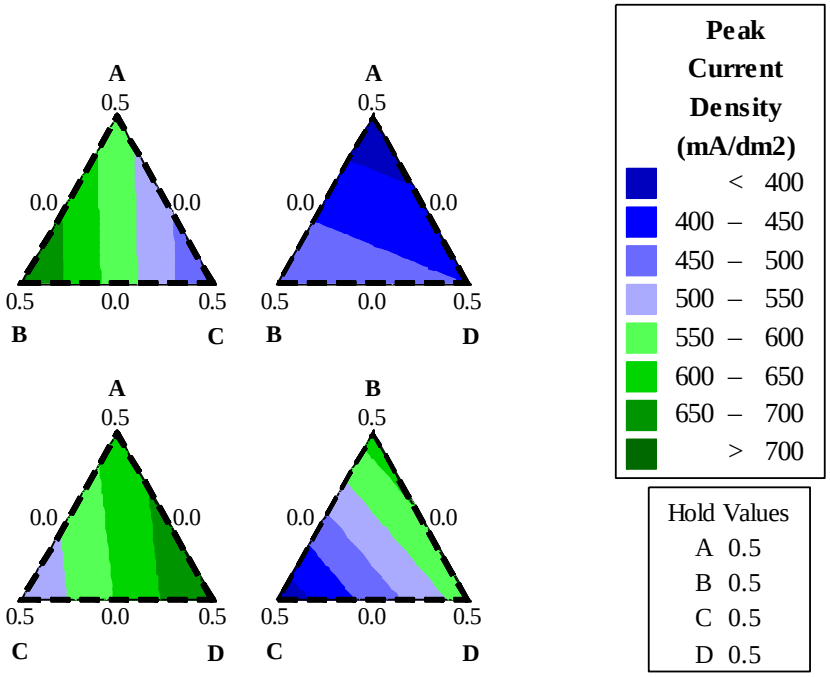

Figure 6. Matrix of mixture contour plots for the peak current densities (mA/dm^2) when surfactant ALS was used. The parameters are; **A** (MoS_2), **B** (Temp.), **C** (pH), **D** (Surfactant).

The contour plots in mixture design analysis given in Figures 5 and 6 show the bands of current densities for the surfactants DC and ALS respectively. The hold value, taken as 0.5, means the middle value of the fourth parameter was used in each plot. For instance; in ABC plot; surfactant (parameter D) was taken as 0.5 g/l which is the mean value of low, 0 and high, 1 g/l levels and for ABD plot, pH

(parameter C) taken as 3 was the average of low, 2 and high, 4 values of pH. The peak current densities were higher than 650 and 700 mA/dm^2 when there was no MoS_2, at pH 2 and temperature 50°C with surfactant 0.5 g/l, as seen in Figures 5 and 6 respectively (corner B of ABC plots). Whereas according to ACD plot of Figure 5; when pH was 2, the peak current density was higher than 650 mA/dm^2 independent of MoS_2 and surfactant concentrations at 40°C. On the other hand, peak current densities were lower than 400 mA/dm^2, when pH was 3 at 30°C in the presence of MoS_2 without surfactant (see corner A of ABD plots of Figures 5 and 6).

4 CONCLUSIONS

The effects of deposition parameters on the peak current density (i_p) for the hydrogen evolution reaction during the electrodeposition of Ni and Ni-MoS_2 composite coatings were studied by fractional factorial design. Interaction effects for the parameters were evaluated including the effects of two commonly used mineral processing surfactants (DC and ALS).

It was found that adding MoS_2, decreasing acidity and decreasing temperature lead to a decrease in i_p for both surfactants. Moreover, addition of the anionic surfactants ALS and DC increased i_p.

ACKNOWLEDGEMENT
The authors acknowledge the Middle East Technical University (METU) for partial support provided through the project BAP-07.02.2010.00.01.

References

1. E. Pompei, L. Magagnin, N. Lecis and P. L. Cavallotti, *Electrochimica Acta*, 54 (2009) 2571
2. N. K. Shrestha, K. Sakurada, M. Masuko and T. Saji, *Surf. Coat.Technol.*, 140 (2001) 175
3. L. M. Wang, *J. Appl. Electrochem.*, 38 (2008) 245
4. Y. C. Chang, Y. Y. Chang and C. I. Lin, *Electrochimica Acta*, 43 (1998) 315
5. M. F. Cardinal, P. A. Castro, J. Baxi, H. Liang and F. J. Williams, *Surface and Coatings Technology*, 204 (2009) 85
6. S. L. Kuo, *J. Chinese Institute of Engineers*, 27 (2004) 243
7. Y. Kunugi, R. Kumada, T. Nonaka, Y.-B. Chong and N. Watanabe, *J. Electroanal. Chem. Interfacial Electrochem.*, 313 (1991) 215
8. P. Berçot, E. Peña-Muñoz and J. Pagetti, *Surf. Coat.Technol*, 157 (2002) 282
9. F. Plumier, E. Chassaing, G. Terwagne, J. Delhalle and Z. Mekhalif, *Applied Surface Science*, 212-213 (2003) 271
10. P. Dabo, H. Ménard and L. Brossard, *Int. J. Hydro. Energy*, 22 (1997) 763
11. R. Santana, A. Campos, E. Medeiros, A. Oliveira, L. Silva and S. Prasad, *J. Materi. Sci.*, 42 (2007) 9137
12. C. C. Hu and A. Bai, *J. Appl. Electrochem.*, 31 (2001) 565
13. C. C. Hu and C. Y. Weng, *J. Appl. Electrochem.*, 30 (2000) 499
14. L. Mirkova, G. Maurin, M. Monev and C. Tsvetkova, *J. Appl. Electrochem.*, 33 (2003) 93
15. T. Fritz, W. Mokwa and U. Schnakenberg, *Electrochimica Acta*, 47 (2001) 55

16. T. Fritz, H. S. Cho, K. J. Hemker, W. Mokwa and U. Schnakenberg, *Microsystem Technologies*, 9 (2002) 87
17. S. Psarrou, P. Gyftou and N. Spyrellis, *Microchimica Acta*, 136 (2001) 159
18. R. A.K.N, *J. Electroanal. Chem.* (1959), 6 (1963) 141
19. L. W. Pan, L. Lin and J. Ni, *Microsystem Technologies*, 7 (2001) 40
20. J. Youngcheol, D. Kiet and K. Chang-Jin, *Micro Electro Mechanical Systems*, MEMS '95, Proceedings. IEEE, (1995) 362
21. L. W. Pan, P. Yuen, L. Lin and E. J. Garcia, *Microsystem Technologies*, 10 (2003) 7
22. S. Gao and A. S. Holmes, *Advanced Packaging, IEEE Transactions on*, 29 (2006) 725
23. A. Ansari and M. Pawlik, *Minerals Engineering*, 20 (2007) 600
24. J. Guo, G. W. Skinner, W. W. Harcum and P. E. Barnum, *PSTT*, 1 (1998)
25. Available from: http://www.surtec.com/kataloge/Electroplating.html
26. A. T. Santhanam and D. T. Quinto, *ASM International*, 5 (1994) 13
27. R. N. Gay and W. K. Raymond, 1988, 4764260 (1988)
28. ASTM and B254-92, 2004, (2004)
29. Minitab Inc. (2007). Meet Minitab 15, State College, PA: Minitab
30. P. M. S. Monk, Linear Sweep and Cyclic Voltammetry at Solid Electrodes, in Fundamentals of Electroanalytical Chemistry, John Wiley and Sons Ltd., England (2001)
31. M. Ibrahim, *J. Appl. Electrochem.*, 36 (2006) 295
32. N. Yamada, H. Shoji, Y. Kubo and S. Katayama, *J. Mater. Sci.*, 37 (2002) 2071
33. J. G. Manjunath, B. E. Kumara Swamy, O. Gilbert, G. P. Mamatha and B. S. Sherigara, *Int. J. Electrochem. Sci*., 5 (2010) 682
34. J. G. Manjunatha, B. E. Kumara Swamy, G. P. Mamatha, U. Chandra, E. Niranjana and B. S. Sherigara, *Int. J. Electrochem. Sci*., 4 (2009) 187
35. B. N. Chandrashekar, B. E. Kumara Swamy, K. R. Vishnu Mahesh, U. Chandra and B. S. Sherigara, *Int. J. Electrochem. Sci*., 4 (2009) 471